JOURNAL OF MATERIALS SCIENCE 37 (2002) 4999–5005

Shape optimization for tool wear in the friction-stir welding of cast Al359-20% SiC MMC

D. J. SHINDO, A. R. RIVERA, L. E. MURR
Department of Metallurgical and Materials Engineering, The Univeristy of Texas at El Paso, El Paso, TX 79968, USA

Tool wear in the friction-stir welding of Al359 + 20% SiC MMC produced a self-optimized shape which when achieved resulted in excellent welds and no additional tool wear. This optimized tool shape was slightly different at weld speeds of 6 and 9 mm/s. Tool wear rate was observed to decrease linearly and to effectively cease above about 11 mm/s weld speed. There was some attrition or comminution of larger SiC particles during welding but the weld zones were very homogeneous in terms of SiC distribution between the base metal and the friction-stir weld zone. There was no weld-related degradation and the weld zone hardness was 30% higher than the base. © *2002 Kluwer Academic Publishers*

1. Introduction

Prado *et al*. [1] have recently described wear phenomena associated with tool consumption and alteration in the friction-stir welding (FSW) of Al6061 + 20% Al_2O_3 MMC. It was observed that the rate of FSW pin tool wear increased up to rotation speeds of 1000 rpm but decreased with increasing weld or traverse speeds. Prado *et al*. [2] have also recently observed a self-optimization of a threaded, hard steel pin tool in the FSW of Al6061-20% Al_2O_3 MMC. This self optimization process produced a pseudohour glass-like or frustum geometry tool shape by abrasive/erosion wear at 1000 rpm rotation speed, and at different weld or traverse speeds up to 540 mm/min. (~21.3 in./min.). When this optimized tool shape was achieved, tool wear (or tool consumption) as determined by shape change essentially ceased.

In the present research program we examined threaded pin tool wear for the FSW of Al359 + 20 vol% SiC MMC in order to confirm the self-optimization phenomenon observed for Al6061 + 20% Al_2O_3 MMC [2], and to compare wear optimized tool geometries and corresponding FSW parameters for Al359 + 20% SiC MMC with Al6061 + 20% Al_2O_3 MMC.

2. Experimental methods

Cast plates (0.4 cm thick), of Al359 (0.2% Cu, 0.5% Mg, 0.2 Ti, 9% Si; balance Al in weight percent) + 20 volume percent SiC particles forming a metal matrix composite (MMC) were variously friction-stir welded by plunging a rotating pin tool into the material. The tool or nib consisted of a 1/4-20, 0-1 AlSl oil-hardened, right-handed tool steel screw, heat treated to RC 62; with a diameter of 0.63 cm and slightly foreshortened relative to the cast plate thickness. A steel backing plate supported the experimental plates to be welded on a milling table of a modified Gorton-Mastermill milling machine. The tool nib was mounted in a 1.9 cm diameter milling chuck which applied a surface shoulder pressure to the workpiece and broadened the FSW zone at this contact surface region. The tool pin (nib) was rotated 1000 rpm since this was observed in the work of Prado *et al*. [1] to exhibit maximum wear. Consequently, we were interested in examining this situation.

Utilizing a photographic technique developed previously by Prado *et al*. [1], the tool wear was measured by comparing standard photographic enlargements of the nib, after specific traverse lengths or FSW passes of 15 cm lengths, with the original nib. This approximate percent of tool wear calculated as tool (volume) consumption was also calibrated by running parallel FSW experiments to specific traverse lengths and then weighing the worn tool for direct comparison with the original tool weight. The effective tool wear in percent of tool consumption (or weight change) was then plotted as a function of traverse or linear weld distance. Cross section samples were also removed at specific locations in the weld plate for optical metallographic examination. These sections were polished and etched with a Keller's reagent consisting of 150 mL water, 12 mL nitric acid, and 12 mL each of hydrochloric and hydrofluoric acid; at 0°C. Rockwell E hardness measurements utilizing a 100 Kgf (1 kN) load were also made across the weld zone samples.

3. Results and discussion

Fig. 1a illustrates the FSW conventions utilized in the FSW experiments and Fig. 1b and c show two examples of weld cross sections at essentially the same traverse (weld) distances. The weld nugget is characterized by the onion-ring flow patterns which became more diffuse with increasing traverse speed (compare Fig. 1b and c). The overall weld zone is also somewhat diffuse as a consequence of the homogeneous distribution of the SiC

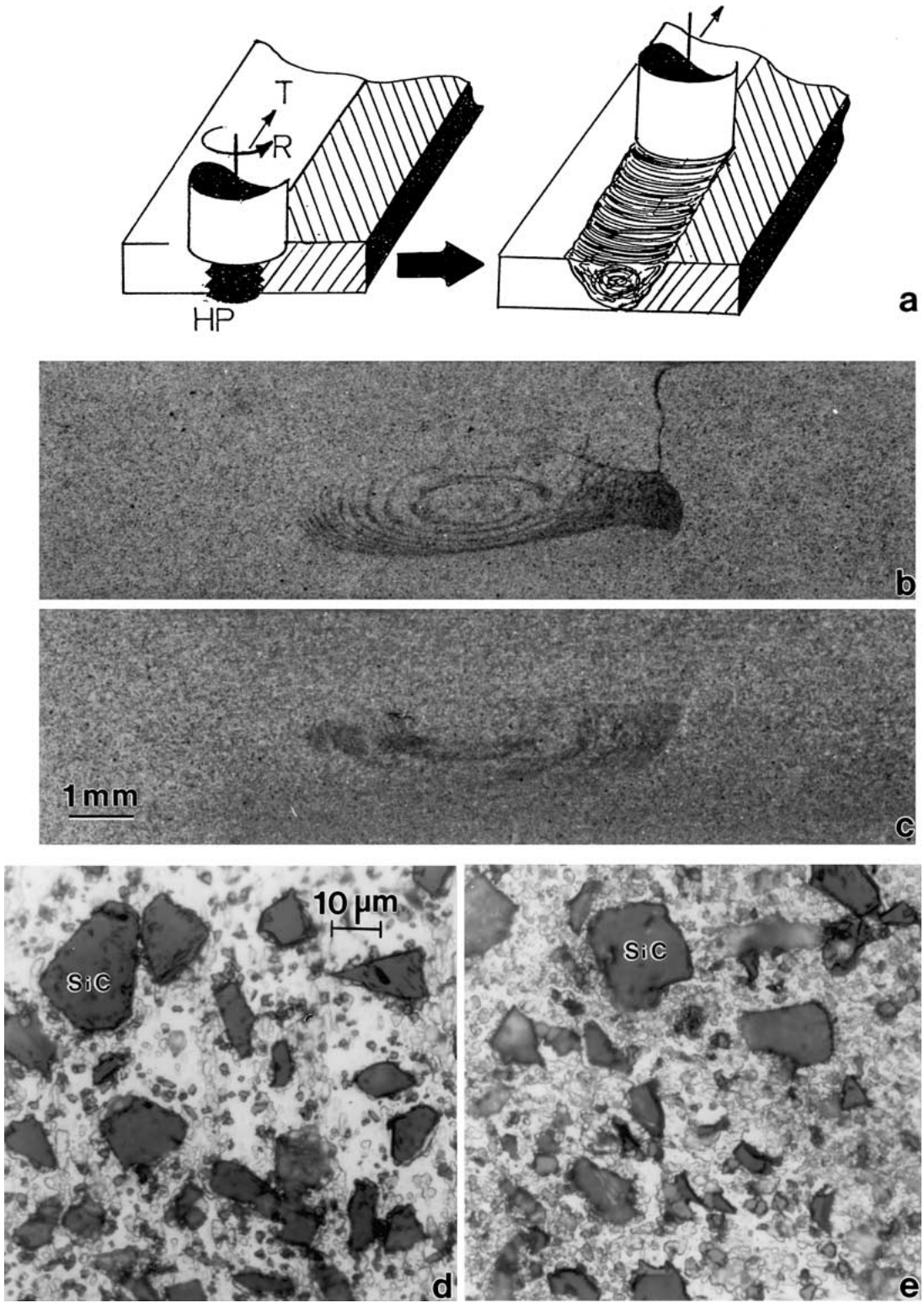

Figure 1 Examples of FSW features and microstructures for Al359 + 20% SiC MMC. (a) Simple FSW process schematic showing weld conventions. The nib (or head-pin (HP) rotates at a speed R and traverses the workpiece material at a speed T. (b) FSW cross-section for weld traverse of 3 cm at $R = 1000$ rpm, $T = 3$ mm/s, (c) FSW cross section for weld traverse of 3 cm at $R = 1000$ rpm, $T = 9$ mm/s, (d) MMC workpiece microstructure showing particle distribution. (e) MMC FSW zone center microstructure in (b).

particles. The details of the workpiece microstructure and that of a typical FSW zone (specifically Fig. 1b) are shown for comparison in Fig. 1d and e. The homogeneous distribution of SiC particles in the workpiece is essentially preserved in the weld zone as noted in Fig. 1b and c. However, as illustrated quantitatively in the frequency (number of particles) versus SiC particle size distribution histogram data in Fig. 2, the size distributions for the workpiece and a FSW zone do change, and the change is characteristic of some attrition or comminution. It can be noted in Fig. 2 that there is a reduction in the very largest particles in the FSW zone while the mean particle size is reduced by 24%; from 4.1 μm to 3.1 μm. The very slight bi-modal distribution in Fig. 2a essentially vanishes in Fig. 2b. This feature (the lack of recognizable SiC particle attrition) has also

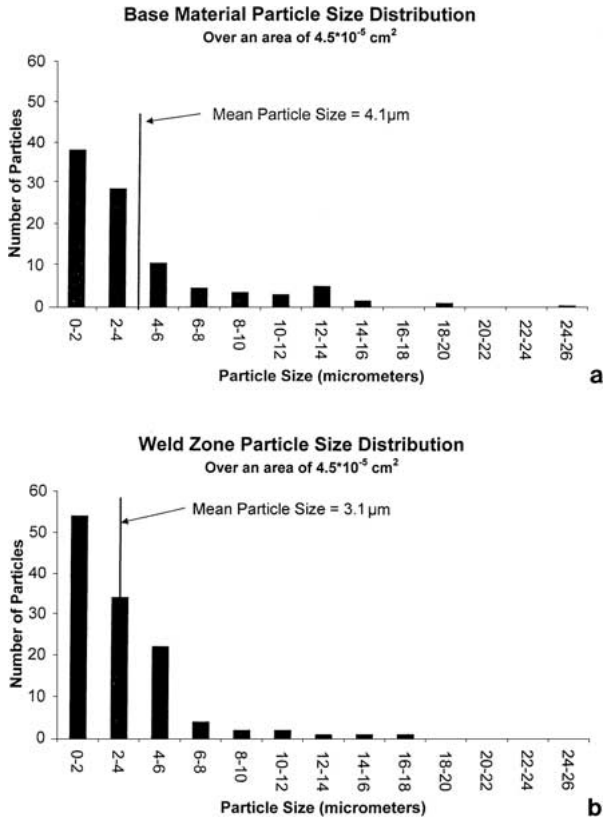

Figure 2 Hitograms for SiC particle size distributions measured for small control areas noted. (a) Base or workpiece, (b) FSW zone ((a) and (b) correspond to Fig. 1d and e respectively).

been observed for FSW of 7093 aluminum + 15 volume percent SiC [3]. However there were no corresponding wear measurements in this work [3].

Fig. 3 illustrates some typical tool/nib wear sequences for different weld speeds. These photographs were used to measure tool (nib or head-pin (HP) in Fig. 1) wear, denoted effective wear percent; measured as a percent of photo weight change from the original tool at zero traverse distance in Fig. 3. The measured effective wear percent is plotted versus traverse or weld distance for weld speeds of 1, 3, 6, and 9 mm/s at 1000 rpm rotation speed, R (Fig. 1a) in Fig. 4. It can be noted in Fig. 4 that the initial slopes of the wear curves decrease with increasing weld speed. Taken together with the tool wear or tool image sequences in Fig. 3, Fig. 4 would suggest that the same tool shapes/wear shapes would emerge at low speeds as those at the higher speeds if the tool were used for longer times or if it traversed correspondingly more material. However, very high initial wear rates may remove enough of the tool volume to make an optimized shape unattainable.

The initial wear rates (in % wear/cm) represented by a straight-line fit to the corresponding curves in Fig. 4—between zero and 100 cm traverse—are shown in Fig. 5 in comparison with the same data for Al6061 + 20% Al_2O_3 particles from the work of Prado *et al*. [2]. While, as noted in Fig. 5, the wear rates for Al359 + 20% SiC are shifted downward in contrast to the wear rate for Al6061 + 20% Al_2O_3, the

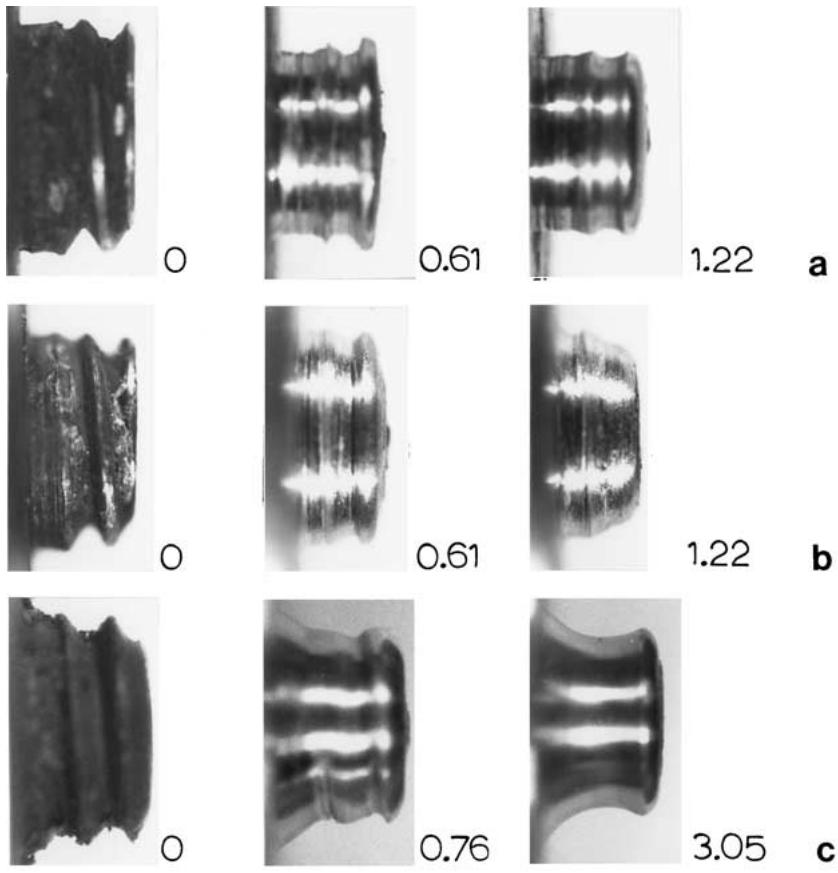

Figure 3 Tool (nib) sequences showing MMC-FSW wear features for constant tool rotation of 1000 rpm and weld traverse distances noted (in meters) for specific weld speeds. (a) $T = 1$ mm/s; (b) $T = 3$ mm/s; (c) $T = 6$ mm/s; (d) $T = 9$ mm/s. (*Continued*.)

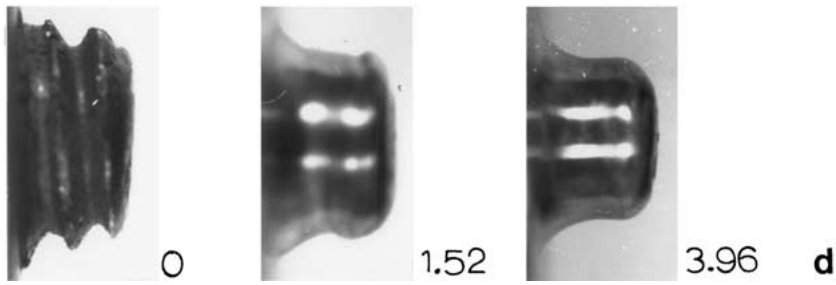

Figure 3 (*Continued*).

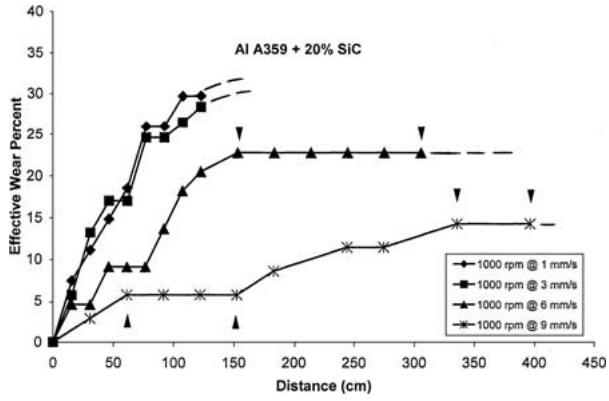

Figure 4 (a) Pin tool wear as a percent of initial nib shape projections (Fig. 3) versus corresponding MMC-FSW linear traverse in cm at various weld speeds noted. Tool rotation constant at 1000 rpm. The arrows on 6 and 9 mm/s curves indicate prominent wearless regimes.

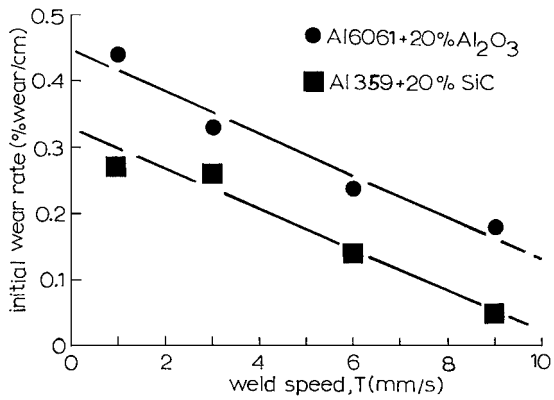

Figure 5 Wear rate (percent wear/cm) versus weld speed or traverse speed, T, from Fig. 4. Data in this study for Al359 + 20% SiC is compared with previous data for Al6061 + 20% Al_2O_3 from Prado *et al*. [2].

slopes are identical. The fact that the tool length for the Al359 + 20% SiC work piece was about 30% shorter than that for the Al6061 + 20% Al_2O_3 may also contribute to this wear data shift in Fig. 5. Extrapolating the data for Al359 + 20% SiC indicates zero wear rate above about 11 mm/s traverse speed (∼26 in./min.).

It is also worth noting that the tool in both the wear conditions depicted in Fig. 5 is subjected to a transient period or a thermal cycle between the 15 cm plate sections. This may produce a more severe wear condition than that which might be achieved by continuous section welding although we do not have any comparative data.

As shown further in Fig. 4, at 6 and 9 mm/s weld speed the wear effectively ceases at sufficiently long traverse lengths (beyond 1.5 m at 6 mm/s and 3.35 m at 9 mm(s). However at 9 mm/s, there appear to be two prominent no-wear plateaus: one between about 60 and 150 cm wear distance, and one beyond about 325 cm. There is also a short plateau between 40 and 75 cm wear distance at 6 mm/s in Fig. 4.

Fig. 6 shows the corresponding tool shapes for the prominent, wearless plateaus in Fig. 4 (marked by arrows). There is essentially no shape change or corresponding wear for the ending plateau regions and the optimal or optimized tool shapes are characteristic of little or no wear. However, the earlier plateau noted at 9 mm/s is not an optimized condition as shown in Fig. 6c and d because the tool exhibits thread wear. Note the shape similarities in the optimized shapes in Fig. 6a and b and e and f. While there is a small shape change between the plateau regions in Fig. 6a and b and e and f, the characteristic frustum-like shape which forms is similar to the self-optimized tool shape recently observed for similar welding conditions in an Al6061-20% Al_2O_3 MMC by Prado *et al*. [2]. Correspondingly, the SiC particles are responsible for the tool (or thread) wear (Fig. 3). The wear occurs by particle erosion/abrasion through translational vortex flow in combination with rotational flow. These flow phenomena erode the tool threads and form the optimized shape, where the tool wear effectively ceases. Fig. 7 provides some simple schematic views of this process which differs somewhat from that shown in the previous work of Prado *et al*. [2] because of the slightly shortened tool with fewer threads as a consequence of the thinner Al359-20% SiC MMC plate. While the vortex flow and overall turbulence is reduced when the self-optimized tool shape is achieved, sufficient solid-state flow persists in order to achieve suitable welds. This alteration in material flow phenomena is reflected in variations in the weld flow appearance illustrated in Fig. 1b and c and an extended comparison in Fig. 8 which compares the onion-skin flow features in the weld face at the early and later stages of welding where the concentric flow features disappear as a consequence of more uniform flow for the shaped (optimized) tool. There are no apparent variations in the weld nugget grain size in Fig. 8 and the differences in appearance do not appear to be related to notable deformation differences.

Fig. 9 also illustrates some changes in the weld features through hardness profile changes corresponding to the conditions illustrated in Fig. 8; for the various weld speeds. It can be noted that, corresponding to the reduction in tool/nib diameter, the width of the weld zone decreases slightly at long traverse distances

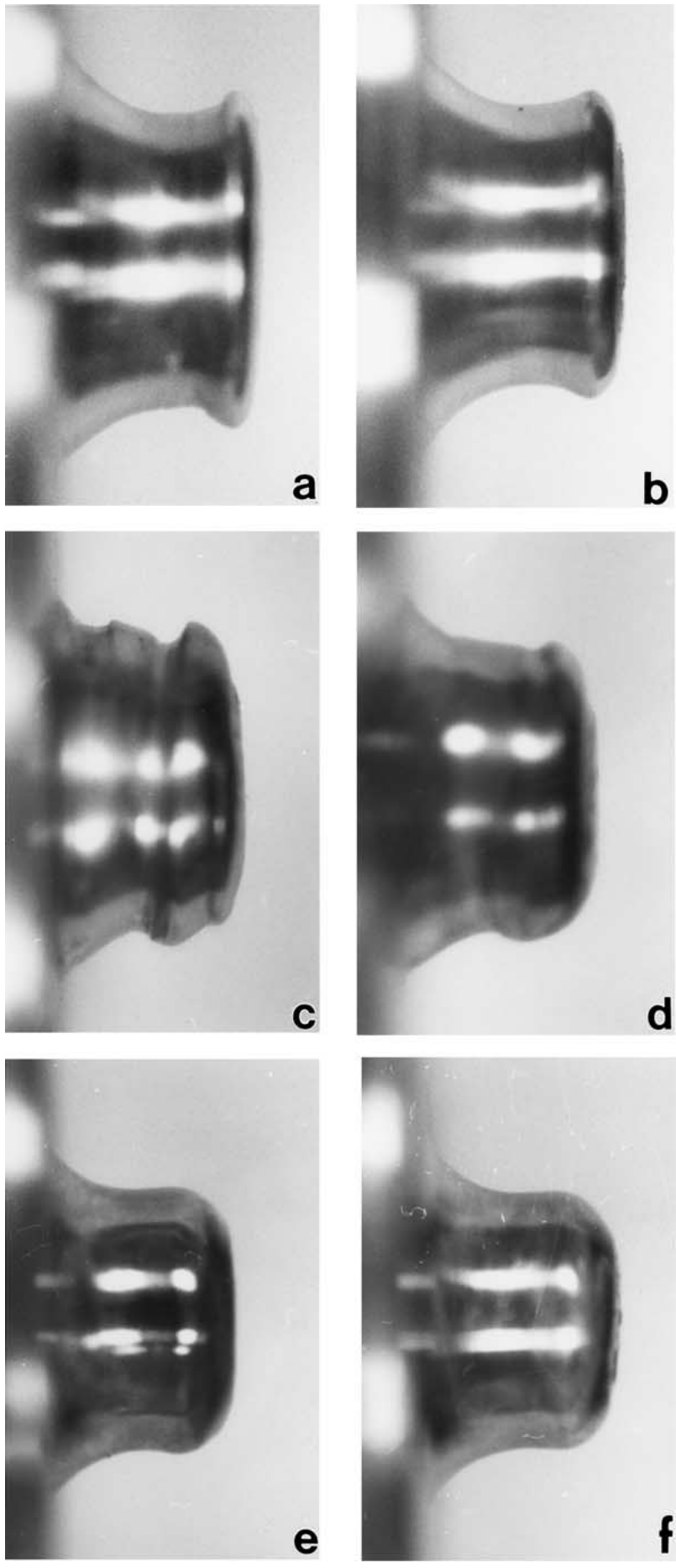

Figure 6 Comparison of self-optimized tool shapes in the region of essentially no wear in Fig. 4. (a) and (b) correspond to linear traverse distances of 2.1 m and 3.1 m respectively at 1000 rpm and 6 mm/s weld speed. (c) and (d) correspond to linear traverse distances of 0.91 m and 1.52 m respectively at 1000 rpm and 9 mm/s weld speed. (e) and (f) correspond to linear traverse distances of 3.35 m and 3.96 m respectively at 1000 rpm and 9 mm/s weld speed (see Fig. 4).

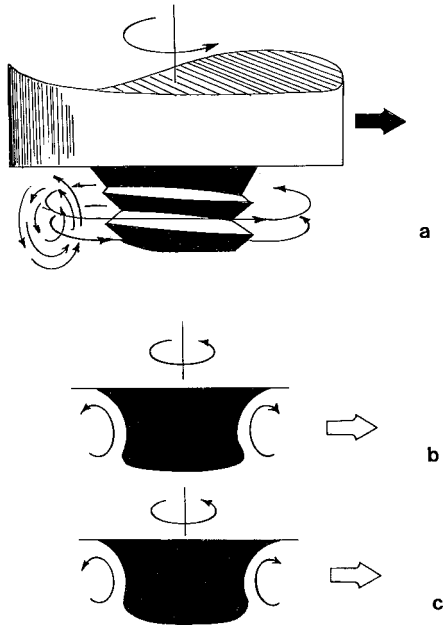

Figure 7 Simple schematic flow diagram for tool wear in MMC-FSW, (a), and shape optimization at 6 mm/s (b) and 9 mm/s (c). Large arrows in (b) and (c) indicate weld traverse direction.

(compare Fig. 9a and b and Fig. 3). We should point out that the specimen width was slightly more than 3 cm.

Consequently the hardness profiles in Fig. 9 do not level off outside the weld zone (including the thermo-mechanically affected zone outside the weld nugget) because of this restricted width relative to the actual weld width. The other interesting feature of the hardness profiles in Fig. 9 is the fact that the weld zone is harder (by roughly 30%) than the base material or workpiece. This of course is in contrast to drops in hardness by roughly 30% for FSW of Al6061-20% Al_2O_3 in the work of Prado *et al.* [2] because of the age-hardening/softening characteristics of that MMC in contrast to the cast Al359 + 20% SiC in this study.

It can be noted in this study, somewhat consistent with the suggestions posed in the work of Prado *et al.* [2] on FSW tool wear for Al6061 + 20% Al_2O_3, that tool designs utilizing slightly curved frustum shapes [4] are probably characteristic of optimized FSW tool shapes for general metals joining, and certainly in joining systems where wear is of serious concern. Additionally, thread or screw-type features need not be included in the tool design since the self-optimized tool (shape)

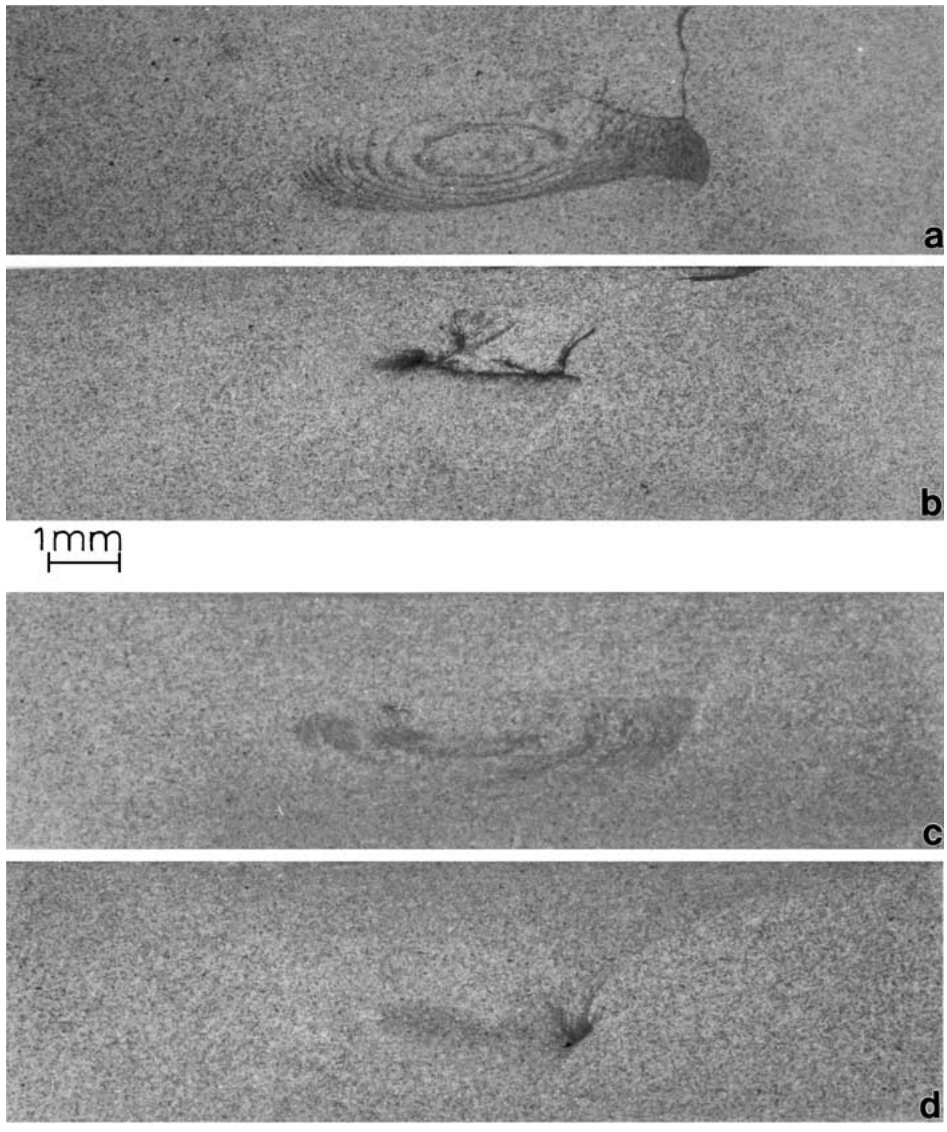

Figure 8 Comparison of the weld zone, cross-section microstructures in the wear region (FSW start) and no-wear or self-optimized tool shape regime of Fig. 4 (FSW end) for a tool rotation speed of 1000 rpm and weld or traverse speeds of 3 mm/s ((a) and (b)) and 9 mm/s ((c) and (d)). The corresponding traverse distances are noted in Fig. 4. Also note the disappearance of the onion-ring flow patterns at the end of FSW.

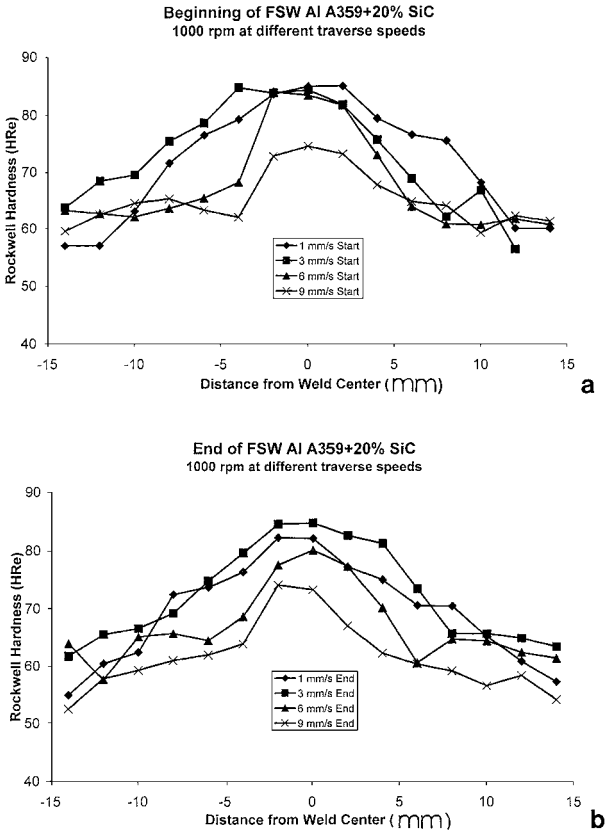

Figure 9 Comparison of MMC-FSW mid-thickness hardness profiles corresponding to initial or beginning wear and reduced or no-wear regimes at the end of FSW in Figs 4 and 8 above; for weld speeds noted. (a) Start of the FSW process corresponding to traverse of roughly 3 cm into the material. (b) End of the FSW process corresponding to end traverse in Fig. 4.

eliminates them, and the resulting welds (made with unthreaded tools as in Fig. 6) are as good or better than those with threaded tools (compare Fig. 9c and b).

4. Conclusions

The FSW of Al359 + 20% SiC MMC using threaded steel pin tools for welding produces a self-optimized shape with no threads which continues to produce excellent, homogeneous welds, but without additional tool wear or shape change at fixed welding speeds above 6 mm/s. This self-optimized shape is slightly different at 6 mm/s and 9 mm/s. Extrapolations of linear wear-rate data indicate zero wear rate above about 11 mm/s weld speed.

Acknowledgments

This research was supported in part by a U.S. Department of Energy Grant DE-FC04-01AL67097 (Amendment No. A0001), a Mr. and Mrs. Maclntosh Murchison Endowment at The University of Texas at El Paso, and a Shell Oil Company Foundation Departmental Grant. We are grateful to David Brown for technical support in friction-stir welding.

References

1. R. A. PRADO, L. E. MURR, D. J. SHINDO and J. C. McCLURE, in "Friction Stir Welding and Processing," edited by K. V. Jata, M. W. Mahoney, R. S. Mishra, S. L. Semiatin and D. P. Field (TMS, The Minerals, Metals, and Materials Society, Warrendale, PA, 2001) p. 105.
2. R. A. PRADO, L. E. MURR, K. F. SOTO and J. C. McCLURE, *Mater. Sci. Engng.*, in press.
3. S. R. SHARMA, R. S. MISHRA, M. W. MAHONEY and K. V. JATA, in "Friction Stir Welding and Processing," edited by K. V. Jata, M. W. Mahoney, R. S. Mishra, S. L. Semiatin and D. P. Field (TMS, The Minerals, Metals, and Materials Society, Warrendale, PA, 2001) p. 151.
4. W. M. THOMAS, E. D. NICHOLAS and S. D. SMITH, TMS Annual Meeting and Exhibition, Aluminum Joining-Emphasizing Laser and Friction Stir Welding, New Orleans, February 11–15, 2001.

Received 26 April
and accepted 9 August 2002